Wet gas flow regime identification based on flow-induced vibration and empirical mode decomposition

Chenquan Hua, Huawei Pan

College of Information & Control Engineering,
China University of Petroleum, Qingdao, China,

Abstract
Flow-induced vibration occurs widely in pipeline transportation system, and the pipeline vibration signals in gas-liquid two-phase flow pipeline have various frequency characteristics corresponding to different flow regimes. Therefore, a novel approach to identify flow regimes for wet gas flow in a horizontal pipeline was proposed, based on flow-induced vibration feature and empirical mode decomposition (EMD). Firstly, the flow-induced vibration signals were collected by a transducer installed on external wall of pipeline. EMD was used to decompose the vibration signal into different intrinsic mode functions (IMFs), and then the normalized energies of each IMF component and the total energy featuring different flow regimes were extracted. Finally, a support vector machine (SVM) classifier, with the normalized feature vector as inputs and flow regimes as outputs, was developed to identify the three typical flow regimes for wet gas flow. The experimental results show that the proposed approach can identify flow regimes effectively, and the identification rate is over 93.4%. The noninvasive measurement approach has great application prospect in online flow regime identification for its advantages of low-cost, riskless and easy to operate.
Key words: FLOW-INDUCED VIBRATION, FLOW REGIME IDENTIFICATION, WET GAS FLOW, EMPIRICAL MODE DECOMPOSITION, SUPPORT VECTOR MACHINE

Introduction

Wet gas flow has been acknowledged as gas and liquid two-phase flow with the percentage of gas volume overwhelming that of the liquid volume. Wet gas flow exists widely in many industrial processes, such as such as nuclear, petroleum, chemical and power equipment industries. Within the oil and gas industry, well fluids with gas volume fraction greater than 90% are widely accepted as wet gas flow[1–3].

Wet gas flow regimes greatly affect metering accuracy, the pressure drop, flow characteristics, heat transfer characteristic, the stability and safety of wet gas flow system[4]. Therefore, flow regime identification is always a fundamental and important topic in the study of wet gas flow. There are three typical wet gas horizontal flow regimes [1,2] in wet natural gas flow productions, including stratified/stratified wavy flow, annular/annular mist flow, and slug flow, as shown in Fig. 1. These flow regimes are caused by the interactions of the liquid and gas, and varies depending on numerous parameters such as liquid and gas velocities, liquid and gas densities, flow composition and many other factors.

There are generally two approaches to perform online flow regime identification. One is invasive approach in which measuring instrument is inserted into pipeline, such as probe method[5] and differential pressure measurement

method [6], etc. The invasive approach has some shortcomings, including flow interference, difficulties in installing and repairing, etc. The other is noninvasive approach which overcomes the above disadvantages from the invasive method, such as high-speed photography, nuclear magnetic resonance, radiation and tomography, etc. For high-speed photography [7], the pipeline in the test section has to be replaced by a transparent pipe, and therefore it isn't applicable to the case where the pressure of the fluid is high, or where the fluid is opaque. For nuclear and radiation principle [8], there is a major security risk.

Flow-induced vibration occurs widely in pipeline transportation system. Flow-induced vibration occurs when wet gas flows through horizontal pipeline, and the pipeline vibration signals have various frequency characteristics corresponding to different flow regimes [9]. Therefore, an alternative novel noninvasive approach to identify flow regimes for wet gas flow is proposed in this paper, based on flow-induced pipeline vibration feature and empirical mode decomposition.

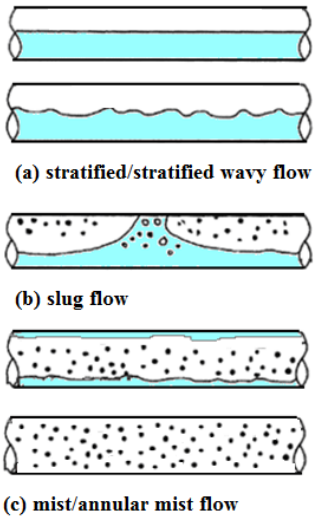

Figure 1. Wet gas horizontal flow regimes

2. Experimental facility and procedure

A series of experiments were performed on the three-phase flow test loop at China University of Petroleum, as shown in Fig. 2. The experiments took air and water as working fluids, and the criterion fluxes of air and water were obtained by a calibrated rotameter and a calibrated Coriolis mass flowmeter respectively. Vibration signals were obtained by a piezoelectric accelerometer sensor installed on external wall of pipeline.

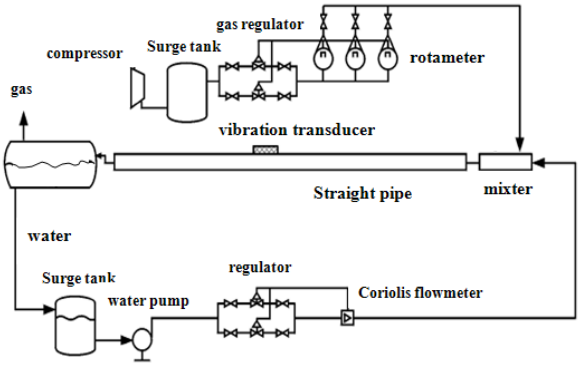

Figure 2. Three-phase flow test loop

The experiments were carried out under the pressure of 0.25MPa in a horizontal pipeline 50 mm in diameter. The gas flow range was 155 ~ 680 Nm3/h, and the liquid flow range was 0.2 ~ 5.3 m3/h. Actual Flow regimes were observed by a transparent window. The designed experimental points are plotted on Mandhane flow regime map [10], as shown in Fig. 3., where Ul and Ug are superficial liquid velocity and superficial gas velocity respectively, which covers 123 groups of data including 70 groups of annular/annular mist flow, 12 groups of stratified/stratified wavy flow and 41 groups of slug flow.

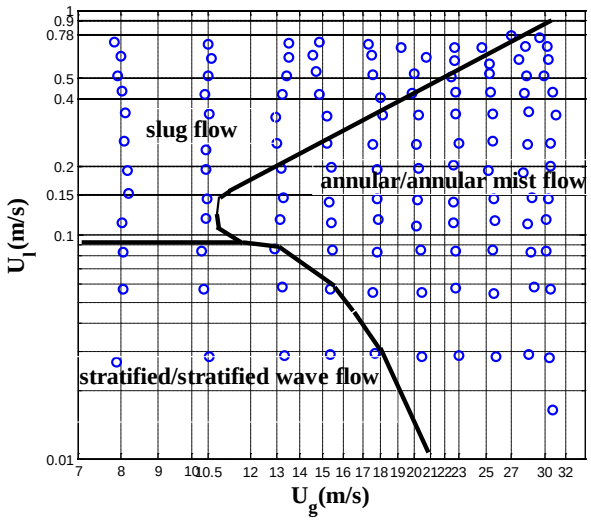

Figure 3. Designed experimental Matrix

3. Flow-induced vibration mechanism

Flow-induced vibration (FIV) would occur due to the existence of flow-induced excitation forces when wet gas flows through horizontal pipeline, and the interaction between pipeline and fluid leads to complex fluid-structure interaction [9]. Therefore, the flow-induced pipeline vibration responses have a closely relationship with flow regimes.

There are three flow regimes for wet gas in horizontal pipeline, as shown in Fig. 1. Fast Fourier transformation is employed to obtain the power spectrums of the vibration signals corresponding to three different flow regimes, as shown in Fig. 4, and it shows that some particular frequency bands of vibration signals become dominant due to various flow regimes. Flow-induced vibration mechanisms for three flow regimes are analyzed as follows:

(1) Stratified/stratified wavy flow

Stratified flow includes stratified smooth flow and stratified wavy flow, as shown in Fig. 3 (a). A smooth interface is formed at the interface of gas-liquid two-phase flow when the gas and liquid phase flow rate are low, and the gas phase flows separately above the liquid phase for the gravitational force on the liquid is dominant. As the gas flow rate increases, the stratified wavy flow is formed at the interface. Power spectrum of a sampled signal for stratified flow is shown in Fig. 4 (a), and the energy values in most frequency bands are small. It is because the gas-liquid two-phase flow rates are low, and the effect of fluid-structure interaction is extremely weak.

(2) Slug flow

As gas flow rate continues to increase, the gas dynamic forces on the liquid phase become strong, and therefore the waves at the interface impact the upper wall of the pipeline regularly, then slug flow is formed. Power spectrum of a signal sample for slug flow is shown in Fig. 4 (b), and the energy values are relatively high in particular frequency band 600Hz~700Hz. According to mechanism analysis of slug flow, it is because liquid hits the upper wall of pipe regularly resulting in a strong effect of fluid-structure interaction at regular intervals.

(3) Annular/annular mist flow

A further increase in gas flow rate leads to a liquid membrane around the inner wall of pipeline with the gas flowing through the center of the pipeline, which is termed as annular flow. If the gas flow rate continues to increase, the liquid membrane will be changed into high-speed mist form by gas dynamic forces, and mist flow occurs. Power spectrum of a signal sample for annular mist flow is shown in Fig. 4 (c), and the energy values are extremely large in particular frequency bands 400 ~ 600Hz, 1600 ~ 1800Hz and 1900 ~ 2000Hz. According to mechanism analysis of annular/annular mist flow, it is because gas dynamic forces play a dominant role in the gas- liquid two-phase flow and gas flow exerts sustained strong force on the liquid flow resulting in a strong and continuous effect of fluid-structure interaction.

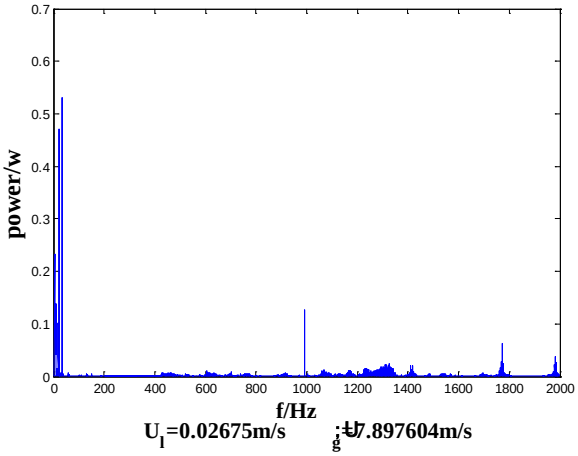

(a) Power spectrums of stratified/ stratified wave flow

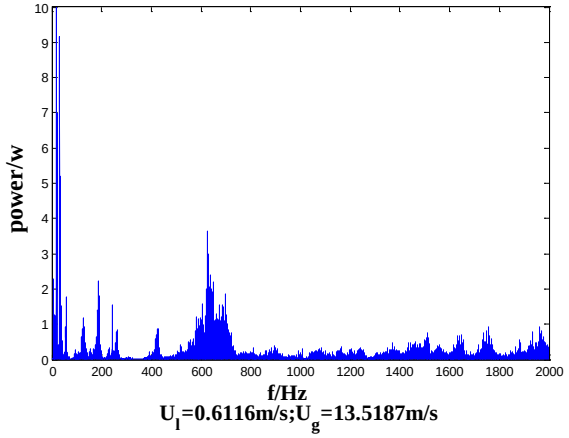

(b) Power spectrums of slug flow

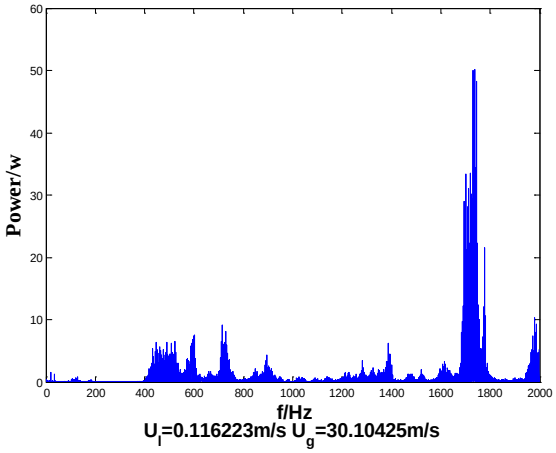

(c) Power spectrums of annular/annular mist flow

Figure 4. Power spectrums of the vibration signal for three flow regimes

Therefore, the frequency characteristics of flow-induced vibration signals are closely related to flow regimes for wet gas. The motive of this paper is to find out the correlation between the above three typical flow regimes and the vibrational characteristics, and then extract flow regime features from the flow-induced vibration signals.

Therefore, the empirical mode decomposition (EMD) is employed to extract flow regime features from the flow-induced vibration signals.

4. Feature extraction based on empirical mode decomposition

The flow-regime dependent vibration signals collected by the vibration transducer are information intensive, but the information hided in signals cannot be extracted from the data straightforwardly. Vibration signals for wet gas flow possess the characteristics of nonlinear, which brings great difficulties to traditional data processing method, such as wavelet transform and Fourier analysis, because the research object of traditional data processing method is linear. To weasel out of this predicament, a new data processing method named empirical mode decomposition (EMD) is adopt to extract frequency characteristic of vibration signals for wet gas flow in this paper [10-14].

4.1 Empirical Mode Decomposition (EMD)

The empirical mode decomposition is a superior method of analyzing nonlinear and nonstationary data, which was proposed by Huang [14]. The basis of empirical mode decomposition is adaptive. The signal is decomposed into so-called intrinsic mode function (IMF) by EMD:

$$x(t) = \sum_{n=1}^{N} IMF_n + r \qquad (1)$$

Where IMF components contain the finest scale or the shortest period component of the signal, and a residue r represent the mean trend or a constant.

The stopping criterion plays a key role in the process of extracting intrinsic mode functions with EMD, and G.Rilling criterion is selected in this paper:

$$\sigma(\mathrm{t}) = \frac{(e_{max}(t) + e_{min}(t))/2}{(e_{max}(t) - e_{min}(t))/2} \qquad (2)$$

Where $e_{\min}(t)$ and $e_{max}(t)$ are the envelopes of minima and maxima, and sifting is repeated until the evaluation function $\sigma(\mathrm{t}) < \theta_1$ for a prescribed fraction ρ, while $\sigma(\mathrm{t}) > \theta_2$ is nonexistent.

It is found that the vibration signals collected by the transducer are nonlinear, and therefore EMD is introduced to extract frequency feathers of vibration signals, which can reflect flow regimes effectively.

4.2 Feature extraction

Feature extraction is considered as the core of flow regime identification, and the features of IMF energy values in different frequency bands of the vibration signals are extracted by EMD. There are three major steps in the process of feature extraction:

(1) The sampling frequency of the vibration signals is 10KHz, and the effective signals frequency range under 2KHz are obtained through fast Fourier transformation de-noising method before feature extraction.

(2) The vibration signal $A(i)(i = 1 \sim 123)$ is decomposed into a finite number N IMF and a residue r with EMD.

(3) The energy of each IMF component is calculated by:

$$E_{i,k} = \sum_{\mathrm{m}=1}^{M} |X_{k,m}|^2 \qquad (3)$$

Where $E_{i,k}$ is the energy of the kth IMF component, and m is the data length of each IMF component.

The energy values of IMF ranging from the fourteenth component to the last one are far less than the energy values of the front thirteenth IMF components, so the sum of the energy values of IMF ranging from fourteenth component to the last one is calculated as the effective energy value of the fourteenth IMF component:

$$E^{\#}_{i,14} = \sum_{k=14}^{N} E_{i,k} \qquad (4)$$

$E_{i,sum}$ is the total energy of all IMF components for experimental series i:

$$E_{i,sum} = \sum_{k=1}^{13} E_{i,k} + E^{\#}_{i,14} \qquad (5)$$

The energy distributions of IMF components for three flow regimes are shown in Table 1, and it implies that the energy distributions of IMF components for pipeline vibration signals corresponding to different flow regimes are obviously different.

Considering the large energy values occurred in each $E_{i,k}$, for the convenience of computation, a normalized operation is performed on the energy of IMF components:

$$E^*_{i,k}=E_{i,k} / E_{i,sum} \quad (6)$$

The normalized IMF energy values of three flow regimes are shown in fig. 5, and the variation trend of the energy distribution of IMF components are different corresponding to three flow regimes. Therefore, such a conclusion can be reached that the normalized energy features can reflect flow regime effectively.

Table 1. Energy distributions of IMF components for three flow regimes

	Energy of IMF															Flow regime
	IMF_1	IMF_2	IMF_3	IMF_4	IMF_5	IMF_6	IMF_7	IMF_8	IMF_9	IMF_{10}	IMF_{11}	IMF_{12}	IMF_{13}	$IMF^{\#}_{14}$	Sum	
1	162.1	45.3	24.7	8.0	3.4	3.4	3.6	13.6	12.2	8.5	2.9	0.4	0.1	0.1	288.3	stratified/ stratified wavy flow
2	202.5	46.1	24.2	8.6	3.6	3.5	3.8	7.7	10.7	14.8	2.1	0.4	0.2	0.2	328.4	
3	348.7	106.4	49.7	11.2	5.7	5.9	3.2	8.4	14.8	20.9	7.5	1.7	0.4	0.4	584.9	
4	17857.3	17750.9	4049.9	2362.3	1737.8	990.4	486.4	1223.1	1328.9	636.5	294.2	31.4	6.9	10.4	48766.8	Slug flow
5	19521.6	19297.7	4278.7	2932.0	2588.2	1109.4	1306.7	1252.9	591.3	256.4	62.8	18.3	3.8	8.1	53227.9	
6	6999.3	6315.4	1852.3	837.6	649.4	400.6	631.5	921.1	647.7	125.9	25.9	9.3	4.0	4.9	19425.1	
7	32877.6	44725.7	7497.6	5545.2	4274.4	1866.2	1438.4	1797.8	707.2	260.2	70.8	23.8	10.9	11.6	101107.5	Annular/annular mist flow
8	33166.5	49086.2	8300.6	6460.1	4665.3	2045.7	2066.7	1925.6	873.7	380.5	92.0	27.2	11.0	18.2	109119.4	
9	24740.6	26018.9	4778.1	3374.9	2435.2	979.6	3353.5	1228.4	480.5	253.4	63.0	12.8	8.4	9.9	67737.1	

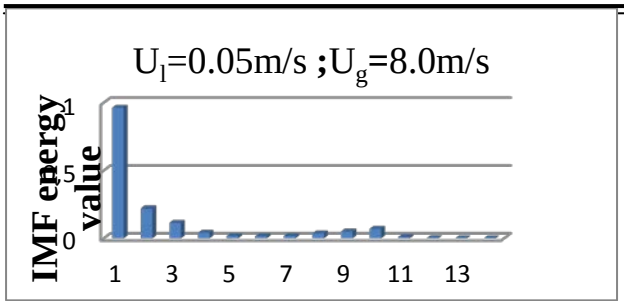

(a) The case of stratified wavy flow

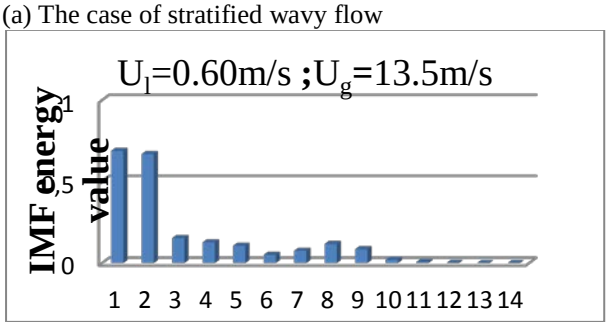

(b) The case of slug flow

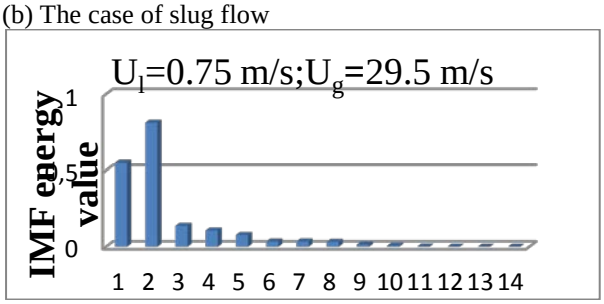

(c) The case of annular mist flow

Figure 5. Normalized energy diagrams of IMF components for three flow regimes

The fourteen normalized energy values of IMF components cannot embody the total energy of various flow regimes effectively. Therefore, the normalized total energy value $E^*_{i,sum}$ is defined as:

$$E^*_{i,sum} = E_{i,sum} / \max\{E_{i,sum}\} \quad (7)$$

Where $\max\{E_{i,sum}\}$ is the maximum value of $E_{i,sum}$ ($i = 1 \sim 123$).

Fig. 6 shows the normalized total energy values of all the experimental data. Two conclusions can be drawn:

(a) Comparing with the total energy values of vibration signals in slug flow and annular/annular mist flow, the total energy values of vibration signals in straight/ straight wave flow are relatively low.

(b) A special phenomenon should be paid attention: the total energy value increases along with the increase of gas flow rate. However, when gas flow rate is fixed, the variation trend of the total energy value with liquid flow rate is significantly different:

For Stratified/stratified wavy flow, the total energy value increases along with the increase of liquid flow rate when gas flow rate is less than 15m/s. However, the total energy value decreases as liquid flow rate increases when gas flow rate is above 15m/s.

For slug flow, the total energy value increases along with the increase of liquid flow rate.

For annular/annular mist flow, the total energy value decreases first and then increases as liquid flow rate increases.

It indicates that the variation trend of the total energy value differs obviously corresponding to different flow regimes. Therefore, the normalized total energy can feature different flow regime.

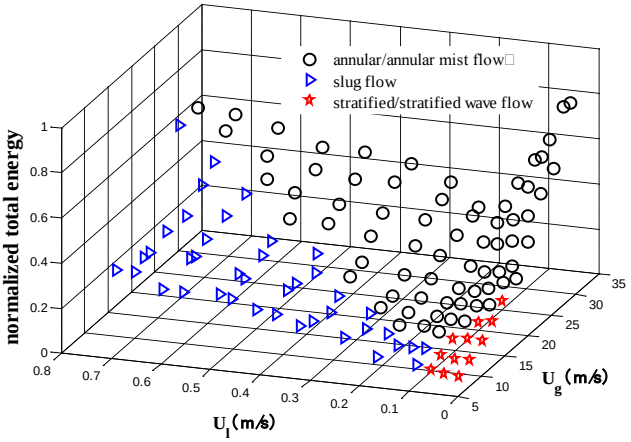

Figure 6. Normalized total energy of vibration signal

Overall, fifteen normalized energy features including fourteen IMF energy features and a total energy feature are obtained for each experimental data, forming a feature vector T^*_i:

$$T^*_i = [E^*_{i,1}, E^*_{i,2}, \cdots, E^*_{i,14}, E^*_{i,sum}] \quad (6)$$

It can be seen that the extracted energy features T^*_i can represent energy distribution of different frequency bands for each vibration signal. Therefore, T^*_i can be used to identify flow regimes for wet gas in horizontal pipeline.

5. Flow regime identification based on support vector machine

The essential of flow regime identification is to implement the nonlinear mapping from

normalized energy feature vector T^*_i to the category of flow regime. However, it is hard to obtain the mathematical relationship between T^*_i and category of flow regime directly. In view of our experiments with smaller samples, the support vector machine (SVM) classifier [15-18] is selected to identify the flow regimes for its advantage of analyzing small data sets and nonlinear data.

5.1 Establishment of SVM flow regime classifier

Flow regime identification is a typical multi-classification problem, and this paper uses one-versus-one classification method to identify three flow regimes for wet gas flow. This method needs to construct $k(k-1)/2$ classifiers, where k=3 is the number of flow regimes in this paper. Each classifier is trained on experimental data from two classes, and therefore three binary classifier including SVM1, SVM2 and SVM3 have to be constructed in this experiment:

SVM1 is trained to distinguish the stratified/ stratified wave flow from annular/annular mist flow, SVM2 is trained to distinguish the stratified/ stratified wave flow from the slug flow, and SVM3 is trained to distinguish the annular/annular mist flow from slug flow.

It deserves noting that 123 groups of data, including 70 groups of annular/annular mist flow, 12 groups of stratified/stratified wavy flow and 41 groups of slug flow, are split into two data sets including the trained data sets with 61 groups and the tested data sets with 62 groups. The number of stratified/stratified wavy flow is relatively less, so 5 groups boundary points of stratified/stratified wavy flow are selected as trained data sets. 35 groups for annular/annular mist flow and 21 groups for slug flow are randomly selected from their own data sets, as shown in table 2.

For example, for slug flow and annular/annular mist flow, the trained data sets of two flow regimes $T^*_{\text{train}} = \{(T^*_1, y_1), \ldots, (T^*_{56}, y_i)\}$ are used as the input to train SVM3 to identify flow regimes, where T^*_i is 15-dimensional normalized energy feature vectors and the output $y_i = \{-1, 1\}$ represents different flow regime. The essential of binary classifier SVM is to implement the nonlinear mapping from normalized energy feature vector T^*_i to y_i, and the decision function is written as:

$$y = \text{sgn}\left(\sum_{i=1}^{l} a_i y_i (K(x, x_i) + b)\right) \quad (7)$$

Where $K(x, x_i)$ is a Gaussian radial basis function $K(x, x_i) = \exp\left(\frac{\|x - x_i\|}{2\sigma^2}\right)$, and Lagrange coefficients a_i is obtained from the following quadratic optimization function:

$$\min_{\alpha} \frac{1}{2}\sum_{i=1}^{l}\sum_{i=1}^{l} y_i y_j \alpha_i \alpha_j K(x_i, x_j) - \sum_{i=1}^{l} \alpha_i$$

$$S.T. \sum_{i=1}^{l} y_i \alpha_i = 0, 0 \le \alpha_i \le C \quad (8)$$

$$i = 1, \cdots, l$$

We have implemented the flow identification by software library for support vector machine (libsvm) [17], which is a simple and easy-to-use support vector machine tool for multi-class classification.

5.2 Process and results of flow regime identification

The tested sets are input to SVM1, SVM2 and SVM3 respectively in order to demonstrate the validity of classifiers, and the voting result is the flow regime. Process of flow regime identification is shown in Fig. 7:

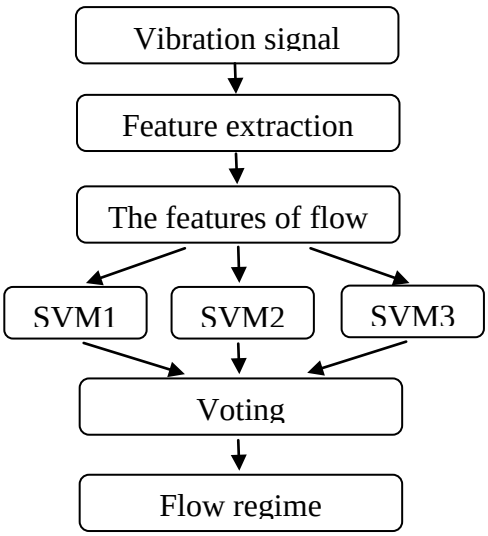

Figure 7. Process diagram of flow regime identification

The 123 groups collected samples were split into two data sets including the trained data sets with 61 groups and the tested data sets with 62 groups. 62 groups of tested data sets were used to verify the effectiveness of the classifiers. The results show that 58 groups from 62 groups of tested data sets are identified correctly, and therefore its total identification accuracy is above

93.4%, as shown in Table 2. There are only four misidentified tested samples, which distribute near the transition zone of flow regimes, as shown in Fig. 8. According to the above analysis, high identification accuracy of flow regime could be acquired in the case of relatively less training samples with the method of SVM. This proved that the proposed SVM classifier has good classification ability for flow regime identification of wet gas flow.

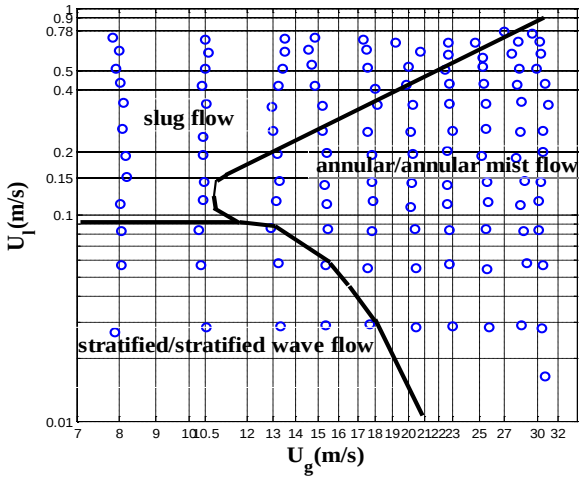

Figure 8. Identified results of test samples

Table 2. Identification results

Flow regime	Trained number	Tested number	Correct number of tested groups	Identified rate of tested groups	Total identified rate
annular/annular mist flow	35	35	34	97.1 %	93.4 % (58/62)
slug flow	21	20	17	85%	
stratified/stratified wavy flow	5	7	7	100%	

6. Conclusion

A novel approach to identify flow regimes for wet gas flow in a horizontal pipeline was proposed based on flow-induced vibration and empirical mode decomposition (EMD). The experimental results show that the flow-induced vibration responses for wet gas flow can reflect the transition between the flow regimes, the extracted feature vector by EMD can reflect different flow regimes, and the trained SVM classifying model can identify flow regimes effectively, and its identification accuracy is over 93.4%. The novel noninvasive approach based on flow-induced vibration can meet industrial needs for its advantages of low-cost, riskless and easy to operate. Therefore, the noninvasive measurement approach has great application prospect in online flow regime identification for its advantages of low-cost, riskless and easy to operate.

Acknowledgment

This work is supported by the National Natural Science Foundation of China under grant 61071041 and 51306212, Shandong Provincial Natural Science Foundation under Grant ZR2012FM012 and ZR2013EEQ033, and the Fundamental Research Funds for the Central Universities Under Grant 11CX04041A.

References

1. Matsubara H, Naito K (2011) Effect of liquid viscosity on flow patterns of gas-liquid two-phase flow in a horizontal pipe. *International Journal of Multiphase Flow*, 37(10), p.p.1277-1281.
2. Zhang L, Wang H.(2010) Identification of oil-as two-phase flow pattern based on SVM and electrical capacitance tomography technique. *Flow Measurement and Instrumentation*, 21(1), p.p.20-24.
3. Mahvash A, Ross A (2008) Two-phase flow pattern identification using continuous hidden Markov model, *International Journal of Multiphase Flow*, 34(3), p.p.303-311.
4. Hua C, Geng Y(2012) Wet gas meter based on the vortex precession frequency and differential pressure combination of swirlmeter, *Measurement*, 45(4), p.p.763-768.
5. Sun B, Zhang H, Cheng L(2006) Flow regime identification of gas-liquid two-phase flow based on HHT, *Chinese Journal of Chemical Engineering*, 14(1), p.p.24-30.
6. Nooralahiyan A Y, Hoyle B S, Bailey N J (1994) Neural network for pattern association in electrical capacitance

tomography. *IEE Proceedings on Circuits, Devices and Systems*, 141(6), p.p.517-521.
7. Zhou Y, Chen F, Sun B (2008) Identification method of gas-liquid two-phase flow regime based on image multi-feature fusion and support vector machine. *Chinese Journal of Chemical Engineering*, 16(6), p.p.832-840.
8. Tambouratzis, T., Pázsit, I.(2009) Non-invasive on-line two-phase flow regime identification employing artificial neural networks. *Annals of Nuclear Energy*, 36(4), p.p.464–469.
9. Blevins, R.D.(1990) *Flow Induced Vibrations*, 2nd edition, Krieger Publishing Company, Malabar.
10. Mandhane J. M., Gregory G. A.(1974) Aziz K., A flow pattern map for gas-iquid flow in horizontal pipes. *International Journal of Multiphase Flow*, 1(4), p.p.537-553.
11. Cheng G, Cheng Y, Shen L, Qiu J, Zhang S (2013) Gear fault identification based on Hilbert–Huang transform and SOM neural network. *Measurement*, 46(3), p.p.1137-1146.
12. Sun B, Zhang H, Cheng L, Flow regime identification of gas-liquid two-phase flow based on HHT, Chinese *Journal of Chemical Engineering*, 14(1), p.p.24-30.
13. Qiangwei L, Baoliang W, Zhiyao H (2007) Flow pattern identification of oil-gas two-phase flow based on empirical mode decomposition and BP neural network. *Chinese Journal of Scientific Instrument*, 28(4), p.p.60-69.
14. Huang N E (2005) Hilbert-Huang transform and its related mathematical problems. *Interdisciplinary Mathematics Sciences*, 5, p.p.1-26
15. Cortes C, Vapnik V (1995) Support-vector networks. *Machine learning*, 20(3), p.p.273-297.
16. Chang C, Lin C.(2011) LIBSVM: a library for support vector machines. *ACM Transactions on Intelligent Systems and Technology (TIST)*, 2(3), p.p.20-27.
17. Fei S.W., Zhang X.B.(2009) Fault diagnosis of power transformer based on support vector machine with genetic algorithm. *Expert Systems with Applications*, 36(8), p.p. 11352–11357.
18. Horng, M.H.(2009) Multi-class support vector machine for classification of the ultrasonic images of supraspinatus. *Expert Systems with Applications*, 36(4), p.p.8124-8133.